



Critical Design Review Report Cover Page & Vehicle Description Form

Human Powered Vehicle Challenge

Competition Location: Digital

Competition Date: February 27, 2021

This required document for all teams is to be incorporated into your Critical Design Review Report. Please Observe Your Due Dates; see the ASME HPVC website and rules for due dates.

Vehicle Description

University name: University of California, Berkeley

Vehicle name: HotDog

Vehicle number: 21

Vehicle configuration:

Upright

Semi-recumbent

Prone

Other (specify)

Frame material: 6061-T6 Aluminum

Fairing material(s): Carbon Fiber and Polycarbonate

Number of wheels: 3

Vehicle Dimensions (m)

Length: 2.87

Width: 1.10

Height: 1.23

Wheelbase: 1.30

Weight Distribution (kg)

Front: 22.3

Rear: 14.9

Total Weight (kg): 37.2

Wheel Size (m)

Front: 0.610

Rear: 0.737

Frontal area (m²): 0.732

Steering (Front or Rear): Front

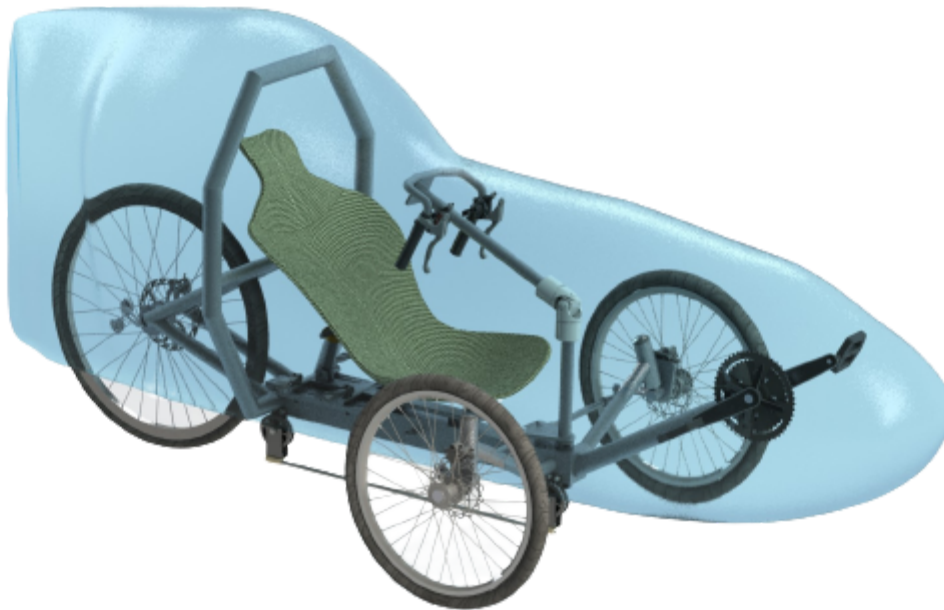
Braking (Front, Rear, or Both): Both

Estimated Coefficient of Drag: 0.1238

Vehicle history (e.g., has it competed before? where? when?): HotDog was designed exclusively for the 2021 ASME HPVC and has not competed before.



University of California, Berkeley
2020-2021 | Design Report
ASME HPVC



Presents

HotDog

Vehicle #21

Dixun Cui

Team Captain

dixuncui@berkeley.edu

Dennis Lee

Faculty Advisor

dennis.lee@berkeley.edu

Aaron Soll

Adam Stewart

Adit Roychowdhury

Benjamin Shoemaker

Cristian Licona

John John Huddleston

Laura Sacristan-Lagunas

Owen Farmer

Rishi Wadgaonkar

Samantha Huang

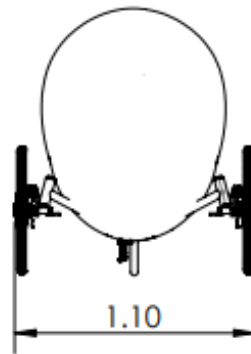
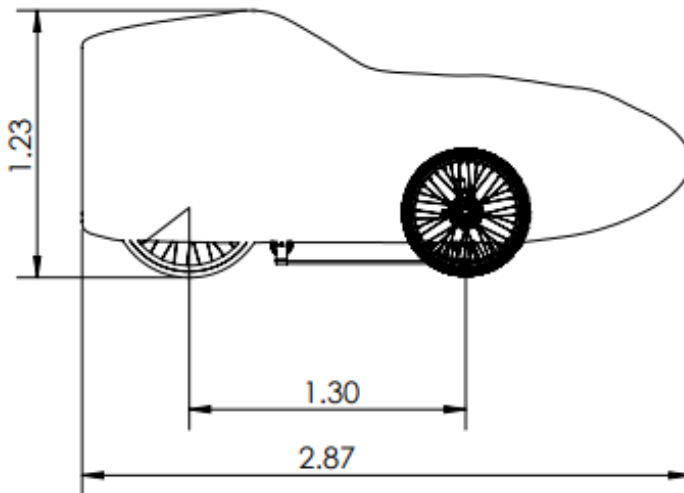
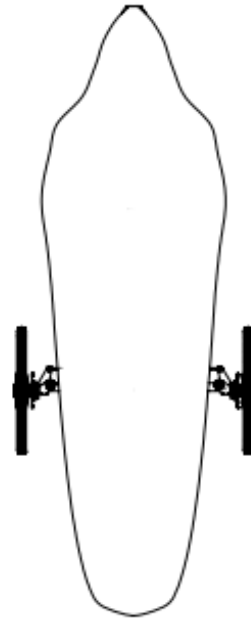
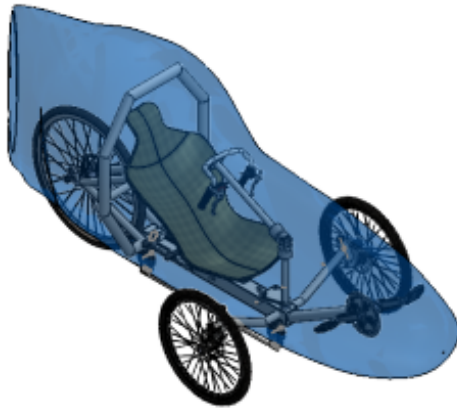
Sara Susanto

Vade Shah

Will Li

Zahra Poonevala

THREE VIEW DRAWING



NOTES:

1. ALL DRAWINGS ARE IN METERS
2. DRAWINGS ARE IN SCALE OF 1:30
3. DIMENSIONING AND TOLERANCING FOLLOW ASME Y14.5 STANDARDS
4. FAIRING SHOWS OVERALL SHAPE WITHOUT ATTACHMENT POINTS AND WINDSHIELD

ABSTRACT

The UC Berkeley Human Powered Vehicle team returns to the ASME Human Powered Vehicle Challenge, after several years away from the event. With a new team and a brand new design, the team aimed to develop a well-rounded vehicle that would be versatile in its use yet effective and structurally sound, all while gaining experience and learning lessons to improve on the vehicle in the future.

Key objectives for our vehicle, HotDog, include sufficient speed, robust safety and reliability, and adjustability to accommodate different riders. Sub-teams were created to focus on different aspects, which included drivetrain, frame, fairing, steering, and safety. All parts were researched and designed during the 2020-2021 academic year by undergraduate students in various technical and non-technical disciplines.

HotDog is a recumbent tadpole trike with an adjustable translating and reclining seat. The vehicle is controlled using an over-seat steering mechanism with Ackermann steering geometry. The compound chainring and internal hub drivetrain allows for 21 different gear settings to allow for versatility and high speeds and torques. The vehicle uses a rear-wheel drive with a robust chain pulley system. HotDog is also fully faired, with a carbon fiber fairing attached to the aluminum frame for enhanced aerodynamics. The fairing contains a windshield for a wide field of view for the driver. Structural safety systems, essential components such as braking mounts and steering mechanisms, and fairing models were all tested with hand calculations and computer simulations to ensure effectiveness and safety. With fresh ideas, the UC Berkeley Human Powered Vehicle team is excited to showcase our newest vehicle design.

TABLE OF CONTENTS

1. DESIGN METHODOLOGY

1.1 Objective	1
1.2 Background	1
1.3 Prior Work	1
1.4 Organizational Timeline	2
1.5 Design Specifications	2
1.6 Concept Development and Selection Methods	2
1.6.1 Drivetrain	2
1.6.2 Frame	4
1.6.3 Steering	5
1.6.4 Seat	6
1.6.5 Fairing	7
1.7 Final Vehicle Description	7
1.7.1 Drivetrain	7
1.7.2 Frame	8
1.7.3 Steering	8
1.7.4 Seat	9
1.7.5 Fairing	10
1.7.6 Safety	11

2. ANALYSIS

2.1 RPS Analysis.....	11
2.2 Structural Analysis	13
2.2.1 Main Horizontal Beam Stress Analysis	13
2.2.2 Back Seat Support Stress Analysis.....	15
2.2.3 Front Arms Finite Element Analysis	15
2.3 Aerodynamic Analysis	16
2.4 Cost Analysis.....	17
2.5 Other Analysis	18
2.5.1 Front Brake Mounts Finite Element Analysis	18
2.5.2 Steering Angles Analysis.....	19

3. CONCLUSION

3.1 Comparison	20
3.2 Evaluation	20
3.3 Recommendation	20

REFERENCES

APPENDICES

1. DESIGN METHODOLOGY

1.1 Objective

For the 2020-2021 academic year, the UC Berkeley Human Powered Vehicle team began a new mission of designing a well-rounded, practical, and efficient vehicle suitable for daily use. The trike is designed with a focus on adjustability and ease of use, while aiming to keep the overall weight low and increase manufacturability. Other goals include designing a stable, accessible, aerodynamic fairing, training new members in design and analysis, gaining experience to ensure longevity, and complying with all ASME rules and regulations.

1.2 Background

HotDog was designed largely using research as a foundation. To learn more about designing human powered vehicles, faculty advisors and alumni were contacted regarding structural analysis and manufacturing techniques. Each sub-team also researched their systems, using resources from past competitions, online manuals, and contacts from our partners at Ford.

By using online resources, we were able to learn more about overall recumbent bicycle design as well as information about specific parts. Sheldon Brown's website was used heavily, with overviews on bicycles as well as articles such as those on internal hubs being very helpful. Significant research was also done regarding tricycle configurations. From looking through past results as well as sites such as LaidBackCycles, the research conducted led to key decisions such as choosing a tadpole tricycle, for published benefits such as stability and weight (O'Brian, 2012).

To gain a better understanding of designing around humans, sport science and cycling resources such as Archibald's *Design of Human Powered Vehicles* were researched, determining that a knee angle around 90 degrees and body configuration angle around 130 degrees would be ideal in a recumbent bicycle for sustained power output (Archibald, 2016).

Research was also done using past reports. UC Berkeley's Super-Gyro report was consulted regarding analysis methods and the overall design process, and SDSU's Quackjack report was studied to better understand part selection and frame design (UC Berkeley, 2018, SDSU, 2019). Overall, the combination of research done about bicycle design, sport science, as well as previous human powered vehicle reports was very beneficial in understanding current vehicle design methods and gaining insight into how to optimize a bicycle for performance.

1.3 Prior Work

No prior work was done that contributed to the design of this year's vehicle. All design elements of the vehicle were newly developed this cycle.

1.4 Organizational Timeline

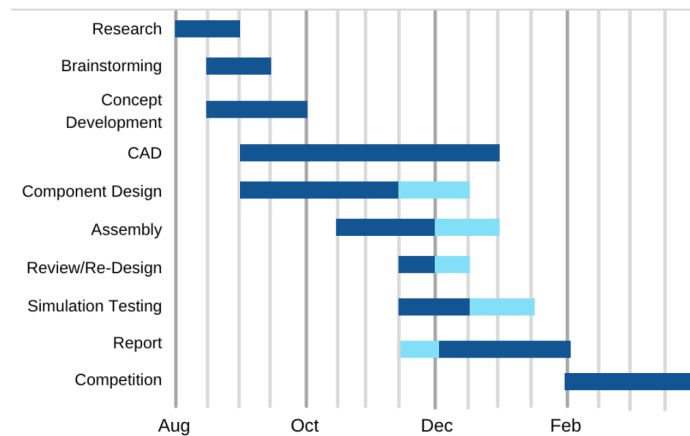


Fig 1: Organizational timeline for HotDog Design. Dark blue bars represent planned working times while light blue rectangles show extra weeks taken

1.5 Design Specifications

To aid in the design process for our bike, we came up with a list of specifications and constraints based on our goals, our past experience, and the competition rules. In order to comply with HPVC rules, the following constraints were set:

1. Vehicle can stop from 25km/hr in 6 m
2. Vehicle can turn within an 8 m radius
3. Vehicle remains stable at 5-8 km/hr
4. Rollover protection system (RPS) can withstand 2760 N top force at a 12° angle from vertical with total deflection below 5.1 cm
5. RPS can withstand 1330 N side force with total deflection below 3.8 cm
6. Vehicle can start without assistance
7. Vehicle has a four or five point safety harness with minimum webbing width of 25 mm
8. All wheels have brakes

In order to be competitive, we aimed for a maximum speed of at least 45 mph. To account for errors in the manufacturing and assembly process as well as unpredictable environmental conditions, we decided to require a minimum factor of safety of 5. To meet the dimensions of many different drivers, we decided to include an adjustable seat. To make room for chain pulleys under the vehicle and account for uneven terrain, we decided to require that the lowest point on the frame is at least 7" above the ground. To reduce drag and increase efficiency, we decided to include a full fairing. Finally, to ensure that we are able to reach high speeds without sacrificing acceleration, we decided to include a minimum of 7 speeds in the drivetrain.

1.6 Concept Development and Selection Methods

1.6.1 Drivetrain

To have effective gearing for both the sprint and endurance races, we want a comfortably wide gear range that can switch between gears very quickly. Shimano makes cassettes in 11-40 and

11-42 gear ratios that come with compatible derailleurs. SRAM also makes a 10-42 cassette that comes with a compatible derailleur, however it requires a proprietary freehub body called a XD driver. Shimano also makes 7 and 11 speed internal hubs that allows the rider to switch gears at a standstill without pedaling. A decision matrix, scoring each category from 1 to 5, was used to evaluate various cassette sizes with respect to speed, adjustability, cost and availability and resulted in the decision to use a 7 speed internal hub from Shimano. This setup will have an acceptable top speed but allow the rider to maintain an efficient cadence at slow speeds while providing high adjustability during various events.

Table 1: Cassette Alternatives

Cassette	Cost	Speed	Adjustability	Availability	TOTAL
Shimano 11x42	4	4	3	3	3.4
Shimano 7 speed internal hub	3	4	5	4	4.0
Shimano 11 speed internal hub	1	3	4	3	3.6
SRAM 10x42	4	4	3	3	3.4
<i>Relative Weighting</i>	<i>10%</i>	<i>30%</i>	<i>40%</i>	<i>20%</i>	<i>100%</i>

One other deciding factor between choosing an internal hub versus a cassette is the availability of discrete gear ratios. Cassettes tend to provide a larger gear range than internal hubs. Subsequently, additional gearing is required with our selected hub to improve its overall range. To accomplish this we decided on using a triple crankset. Although this adds an additional derailleur for the rider to manage, it is a simple solution that allows us to meet our speed requirements while also meeting our agility requirements by allowing the rider to shift gears while stopped.

Since our recumbent trike utilizes a tadpole configuration with a rear drive, we needed to design a chain routing solution to efficiently transfer power from the pedals to the rear wheel with proper tensioning and as little friction as possible. From competitor and consumer product research, we made the consensus to use toothed pulleys with a straight tube routed directly underneath the driver. This provides stable, convenient mounting options due to the location of the main rectangular beam and minimizes angular displacement of the chain from the bike's loaded areas. The components we chose are also either easily fabricated in-house from raw materials or purchased from a third party supplier that specializes in professional grade recumbent trikes. Table 2 explains some of the components chosen and their justification.

Table 2: Drivetrain Component Justification

Category	Choice	Justification
Gearing	Shimano Nexus 7-speed internal hub w/ 16t cog	Determined by decision matrix.
Crankset	Shimano Tourney A073 170mm 30 x 39 x 50t 7/8-Speed Triple Crankset	Provides good range of gear ratios in a compact and lightweight solution.

Table 2 (Continued)

Front Derailleur	Shimano Tourney A073 7-Speed Triple Front Derailleur	Requisite for selected crankset.
Chain	SRAM PC-830 8 Speed Chain	Compatible with crankset and internal hub. Weight benefits of higher speed negligible considering compatibility.
Pulleys & Chain Routing	½" OD x ⅜" ID Delrin Acetal Resin Tube and 100mm diameter SportPlus 23 Tooth Idler	Tubing provides easy routing of the chain to prevent sagging with minimal frictional losses. Large pulleys improve efficiency and durability at high speeds.
Mounting	.125" 6061 Aluminum Plate machined into custom bracket	Laser cut sheet metal allows for easy design of custom brackets for our unique frame.
Back Tensioner	Shimano Alfine Chain Tensioner	Compatible with our internal hub and applies ample chain tension.
Wheels	29" Rear Wheel Drive	Larger drive wheel increases max speed and reduces friction compared to smaller wheels.

1.6.2 Frame

The first decision to be made regarding the overall frame design was the type of human powered vehicle, where the main options were tadpole tricycle, delta tricycle, and two-wheel recumbent bicycle. We ranked each of these styles in four categories-- speed, handling, ease of assembly, and safety in a decision matrix. Each of these categories were then given a relative weighting corresponding with the extent to which we wanted to consider each one in our final decision. In order to provide a reliable and non-arbitrary basis of comparison, all rankings are relative to each other. Rankings are awarded 1 to 5 points, with 5 being awarded to the style of vehicle that is best in each category. We then totaled the weighted points for each type of vehicle and selected the type of vehicle with the highest total.

Table 3: Type of Human Powered Vehicle Design Alternatives

HPV	Speed	Handling	Ease of Assembly	Safety	TOTAL
Tadpole Trike	3	3	3	5	3.6
Delta Trike	2	4	2	5	3.3
2 Wheel	4	1	4	2	2.8
<i>Relative Weighting</i>	30%	20%	20%	30%	100%

Thus, our relative preference for speed while maintaining solid maneuverability led us to a tadpole tricycle design. We used this same decision-matrix method for deciding on a material for the chassis; for this decision, we considered aluminum, carbon fiber, steel, and titanium. The characteristics we considered were durability, ease of manufacturing, cost, and weight.

Table 4: Material Alternatives

Material	Durability	Ease of Manufacturing	Cost Effectiveness	Low Weight	TOTAL
Aluminum	2	4	4	5	3.9
Steel	4	5	4	1	3.4
Titanium	3	1	2	2	1.9
<i>Relative Weighting</i>	20%	30%	20%	30%	100%

As seen above, our strong preference for a light and manufacturable material led us to use aluminum for the chassis. At this point, a few final big-picture decisions were left to be made regarding the frame: type of brakes, rear-stay geometry, and the rollover protection system geometry. Since there were not a discrete list of options and considerations for each of these components, the decision matrix methodology did not make sense. Table 5 shows each of these decisions and their justifications.

Table 5: Component Choices and Justification

Component	Choice	Pros	Cons	Justification
Brakes	Disc Brakes	Offer greater stopping power, more precise breaking, and are more reliable	Can be heavier, more expensive, and more difficult to mount than a rim brake alternative	Overall, the higher reliability and precision of the disc brakes makes them a safer option for a vehicle traveling at high speeds.
Rear Stay Geometry	Triangulated Stays	Better at distributing force, significantly more stable	Higher weight, more material, and harder to manufacture	From a safety aspect, the extra weight and material was deemed a minor inconvenience due to the necessity of having a sturdy rear wheel geometry.
RPS Geometry	Roll Cage Around Shoulders	Offers full protection for shoulders, head and spine in the event of rollover	Would be heavier and involve multiple weld joints	A full RPS was deemed to be worth the extra material, as it drastically increases the safety of the vehicle.

1.6.3 Steering

Determining the steering mechanism used by HotDog was a two step process. The first was to narrow down the general type of steering from over seat, under seat, or direct knuckle using the design matrix method. Over seat steering was optimal due to its intuitive user experience (similar to driving a car), and its ability to be compactly integrated into our design without interfering with the seat or fairing.

Table 6: Types of Steering Design Alternatives

Steering Type	Weight	Manufacturing	Ergo: Seat	Ergo: Fairing	User Experience	Total
Over seat	3	3	3	5	4	3.6
Under seat	2	3	2	3	3	2.6
Direct knuckle	3	4	2	1	3	2.5
<i>Relative Weighting</i>	<i>10%</i>	<i>20%</i>	<i>30%</i>	<i>20%</i>	<i>20%</i>	<i>100%</i>

The next consideration was the linkage system used in the over seat steering design. Different possible steering linkages, as well as their pros and cons in conjunction with an over seat steering design, were analyzed using information from Rickey Horwitz's pdf, *The Recumbent Trike Design Primer*. A dual drag linkage system was chosen due to its simplicity, low weight and part count, and its compact nature, making it work extremely well with an over seat steering system and causing little interference with the fairing (Horwitz, 2010).

Table 7: Steering Linkage Configuration Design Alternatives

Linkage Configuration	Weight	Manufacturing	Spacing	Ergo: Steering Sys.	Reliability	Total
Single tie rod and drag link	3	4	3	3	4	3.4
Dual drag link	3	3	4	5	3	3.8
Crossed dual drag link	2	2	2	3	4	2.7
<i>Relative Weighting</i>	<i>10%</i>	<i>20%</i>	<i>20%</i>	<i>30%</i>	<i>20%</i>	<i>100%</i>

In addition to the general steering mechanism, several different handlebar designs were considered. The primary concern was that, for both safety and ease of use, the rider had to be able to work the gear shifters as well as the brakes without having to move the position of their hands on the handlebar. The handle bar design shown in figure 2 allows riders to brake with their fingers, shift with their thumbs, while at the same time turn the handlebars radially to twist the U-Joint, as described in the steering description section.

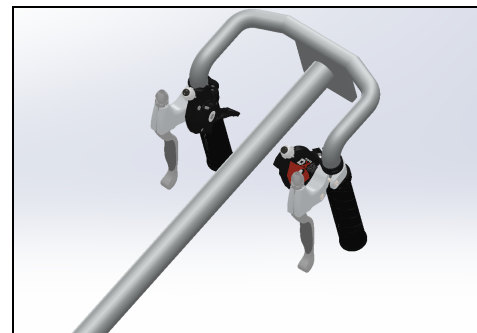


Fig 2: Handlebar Assembly

1.6.4 Seat

The seat material was an important factor to consider and a decision matrix was used.

Table 8: Seat Material Design Alternatives

Material	Weight	Manufacturing	Ergo	Reliability	Total
Foam	5	2	3	1	2.6
Carbon Fiber	3	3	3	4	3.3
Plastic	3	2	2	4	2.9
<i>Relative Weighting</i>	<i>25%</i>	<i>25%</i>	<i>20%</i>	<i>30%</i>	<i>100%</i>

We decided on carbon fiber for our seat material, as shown in Table 8. We also decided that since the bike needed to be ridden efficiently and effectively by multiple riders of different heights, the seat needed to be able to translate forwards and backwards along the bike. Thus, we decided that some seat attachment system would need to be implemented. The seat attachment system needed to satisfy 3 important criteria: sturdiness for the axial load of the rider, adjustability for different riders, and proper implementation to prevent backlash between components. Final seat designs are outlined in section 1.7.4.

1.6.5 Fairing

There are many popular fairing designs such as full, front and rear fairings. In order to shield the rider from all weather conditions we selected a full fairing over the other styles of fairing, as they are unable to provide this level of protection. With the full fairing it is critical that the weight of this component is minimized. In order to meet this objective we selected carbon composites for their strength to weight ratio. As the fairing goes through testing and transport it is likely to scrape against the ground despite careful handling, an outer lamina of kevlar carbon hybrid weave will be added to the laminate stack to increase the durability of the fairing. In designing the windshield, we considered it a non-structural component and therefore decided on using thin lexan polycarbonate as the material because it can be modified into the shape we designed and is clear which is necessary to give the driver a clear view of their front path.

1.7 Final Vehicle Description

HotDog is a tadpole recumbent trike designed with the goals of versatility, speed, and safety. With a full carbon fiber fairing, it is designed to handle mild weather conditions and terrains in day-to-day use. Specific component descriptions are provided below.

1.7.1 Drivetrain

HotDog is using a Shimano Nexus 7-speed internal hub w/ 16t cog in the 29" rear wheel linked to a Shimano Tourney A073 170mm 30 x 39 x 50t 7-Speed Triple Crankset in the front drive. The chain is the SRAM PC-830 8 speed chain, which is compatible with both the internal hub and triple crankset, while allowing easy replacement and length adjustment due to the "Powerlink" feature. The front derailleur is the Shimano Tourney A073 7-Speed Triple Front Derailleur which matches the front crankset. The rear tensioner is a Shimano Alfine Chain Tensioner, which is compatible with the internal hub and keeps our chain properly tensioned consistently. The drivetrain assembly is shown in figure 3.

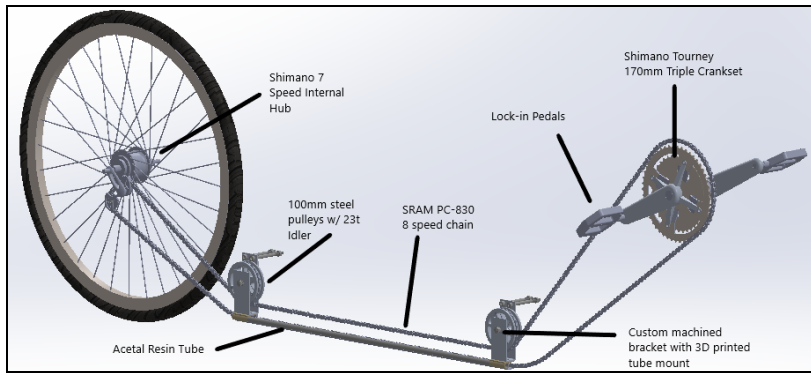


Fig 3: Chain routing assembly with pulley and tube system

For chain routing, HotDog is using a single $\frac{1}{2}$ " OD x $\frac{3}{8}$ " ID Delrin Acetal Resin Tube and dual 100mm diameter SportPlus 23 Tooth Idlers to efficiently transfer power to the rear wheel with as little power lost to friction and lack of tensioning as possible. Both the pulleys and the tubing are mounted using a custom bracket machined from .125" 6061 Aluminum sheets and 3D printed components, fastened to the large square beam of the frame.

1.7.2 Frame

HotDog has a sturdy frame made from aluminum tubes of different sizes. A square 3" x 3" aluminum tube was used as the base, as opposed to a circular tube, for several reasons. First, the aluminum plate used for the seat attachment and adjustment needed to be balanced on a long, flat surface for ease of manufacturing and better stability. In addition, the flat faces of the square tube would make it easier to drill holes for the front wheel arms and roll cage tubes, as well as make it slightly easier to mount the chain pulleys at the bottom. The frame geometry was determined based on a CAD model of our largest rider. Disc brakes are on all three wheels, with calipers that are attached to front mounts and the back wheel stays.

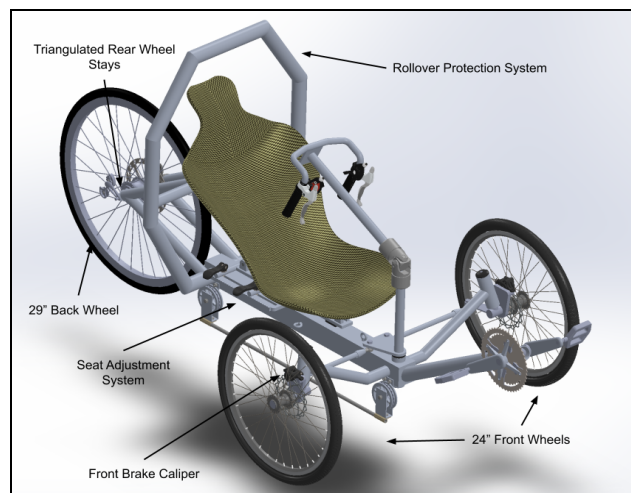


Fig 4: Full Assembly

1.7.3 Steering

HotDog uses an over seat dual drag linkage steering system, similar to a rack and pinion system but with a bell crank instead of gears. A diagram with labeled parts is shown in figure 5. Tie rods connect a central bell crank to the steering knuckles attached to each wheel. The bell crank is then welded to the steering shaft,

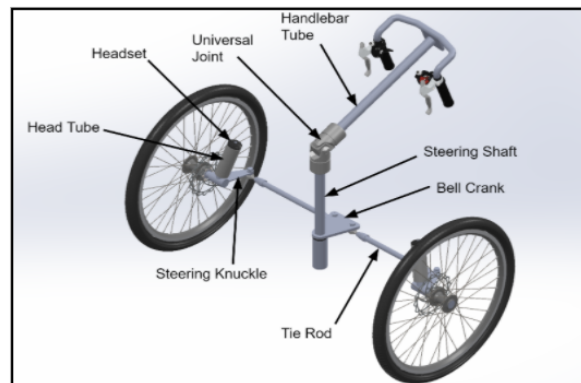


Fig 5: Steering Assembly

which in turn connects to the handle bar tube with a universal joint. When the handlebars are turned radially, the U-joint allows for the rotational motion to be transferred to the bell crank despite the handlebar tube being misaligned with the steering shaft. For stability, a small head tube is fitted into the frame, in which integrated bearings allow the steering shaft to smoothly rotate with minimal play, much like the kingpin assembly.

Steering geometry was also considered. We strived to achieve as close to a 100% Ackermann compensation as possible within manufacturing limitations. Therefore, the steering knuckles are aligned with the rear wheel axle so that the inner wheel turns at a tighter angle than the outer wheel, preventing scrubbing. As far as the steering geometry, we set a 15° kingpin angle, a 10° caster angle, and a neutral camber. Specific information can be found in Appendix B.

1.7.4 Seat

The body orientation angle, knee angle, and hip orientation angle we chose were 130, 91 and -5 degrees respectively, based on Archibald's *Design of Human Powered Vehicles* (refer to Appendix F). These angles match with our tallest rider.

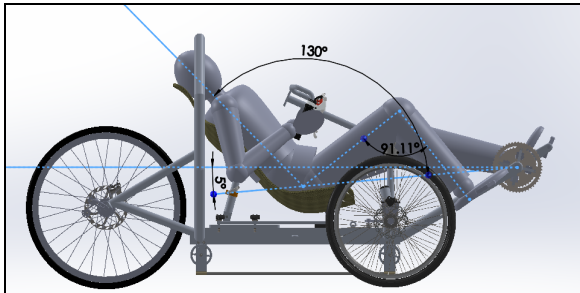


Fig 6: Seat with rider body angles

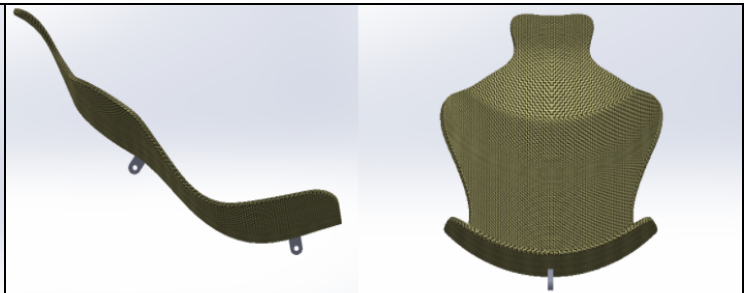


Fig 7: Overall Seat Images

Using the design criteria outlined in section 1.6.4, we first determined that the most effective way to fasten the seat attachment system to the chassis was through a metal plate welded to the central beam; adding this metal plate would prevent holes from being drilled into the central beam, which transmits most of the load of the rider. Our design allows for two different degrees of freedom: translational freedom forwards and backwards along the bike, and rotational freedom to change the angle of the seat. This rotation would allow for the smallest possible angle of the rider relative to the horizontal, regardless of the rider's height.

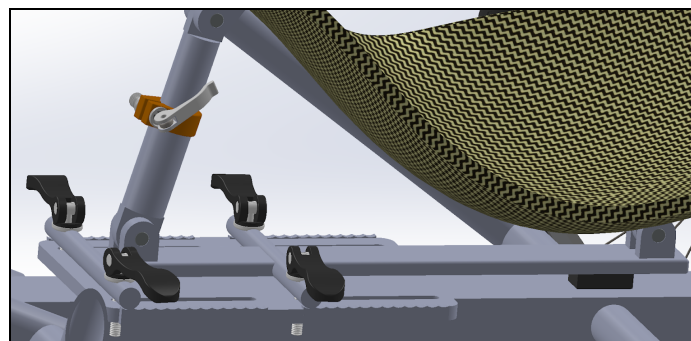


Fig 9: Overview of the Seat Attachment System

To allow for translation of the seat, we used aluminum tubes which would slide forward and backward and lock into discrete locations with the use of four large cam levers, seen in figure 9 in black. Similarly, a post clamp was selected to allow the seat to rotate once it is moved to a new position. This post clamp, seen in figure 9 in orange, works similarly to the seat adjustment clamp in most commercially available upright bikes. All connection points are pinned to allow appropriate angles to change when the bike is adjusted.

1.7.5 Fairing

The primary function of the fairing is to reduce the drag forces experienced by the vehicle. In order to reduce the coefficient of drag, the shape of the fairing is designed first with aerodynamic principles and then is validated using CFD simulations. By reviewing past designs and communicating with alumni of the club, it was determined that a coefficient of drag less than 0.2 is sufficient to benefit the vehicle. The fairing is considered a nonstructural component and a three lamina carbon weave construction with an outer layer of kevlar-carbon hybrid weave is enough to support itself. While this is strong enough to hold together, Nomex honeycomb with a layer of carbon weave will be added to stiffen the fairing in select regions. The next design consideration is rider entry and fairing attachment to the vehicle. In order to allow for this functionality, the fairing will be broken up into three main components: the rear base, front base, and the top. The rear base and front base will be attached to the frame in a semi-permanent method using 3D printed brackets. The top however can't be attached in this way, as the removal of this element is how the rider is able to exit the vehicle. For safety reasons, we determined that the top element should be able to be opened by both the rider or by someone outside the vehicle. In order to achieve this, vertical slots are bonded into both of the base components and vertical pegs are added to the top component. Then a packing tape seal can be added to close and secure the gap between the base and top components after the rider has entered the vehicle. The top component also contains the windshield and this component is bonded to the top component by the use of an epoxy paste and small brackets.

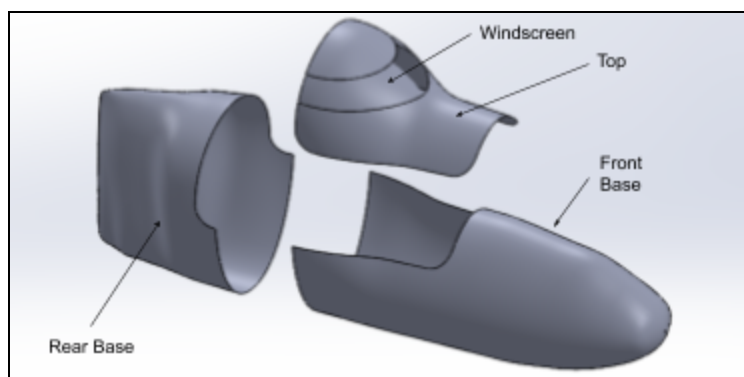


Fig 10: Fairing Component Exploded View

The last features of the fairing revolve around areas to be cut out to allow for clearances of other components of the vehicle. In the rear, a hole is cut to allow for the wheel to touch the ground. Relatively small holes are also cut into the side of the fairing to allow for the steering linkages and the front wheel supports. A slot is also cut on the bottom of the fairing in order to

allow for the low-hanging chain pulley system to not interfere with the fairing. Note these hole elements are not visually depicted on the fairing image in figure 10. These holes are also considered small enough and located in areas which minimally affect the drag coefficient of the vehicle.

1.7.6 Safety

Safety is one of HotDog’s biggest priorities. Both four and five point harnesses were considered as safety harness options. While a five point harness required drilling an extra hole into the frame to mount the harness attachment fixture, we decided this was worth it to prevent the rider from sliding forward in their seat during a collision. Following proper safety protocols, it is recommended that harnesses be attached to the vehicle by clipping the lap straps onto grade 8 eye bolts and by looping the shoulder straps onto a cross bar roughly at shoulder level in order to prevent spine compression (Krider, 2018). Thus, HotDog has three grade 8 eye bolts welded into the square bottom tube: two on the sides for attaching the lap harness straps, and one on top, in front of the seat, for attaching the front strap of the five point harness. The shoulder straps are looped around the crossbar of the RPS. Although they are slightly lower than shoulder height, due to the reclined position of the rider, versus an upright position of someone sitting in a car seat, there is less force directed along the rider’s spine. To maximize safety, a commercial automobile harness as opposed to a self-fabricated harness is used, with specifications given in Table 9.

Table 9: Commercial Safety Harness Specifications

Manufacturer	Description	Strap Width	Material	Safety Rating
Jegs High Performance Parts	Black Cam Lock Ultra Series 5-point	3 in.	Nylon	SFI 16.1

In addition, the rest of the HPV is also designed with safety in mind. All open ends are covered, edges are filleted, and the hands are away from any dangerous pinch points. Plenty of space is given for the rider’s helmet, and the fairing has a clear windshield, allowing for a field of view greater than 180 degrees.

2. ANALYSIS

2.1 RPS Analysis

Table 10: Summary of RPS Analysis

Criteria	Description
Objective	Verify the safety of the RPS by testing top load and side load cases
Method	Solidworks FEA simulation
Final Result	A 2” diameter, 3/16” wall thickness aluminum tubing was used, resulting in a minimum factor of safety of 5.3

2.1.1 Objective

The rollover protection system (RPS) is designed to protect the rider during the event of a rollover or crash. In order to ensure the highest safety of the rider, the RPS is made from thick aluminum tubing attached to the frame and completely encompasses the rider's head, neck, and shoulders. In order to evaluate the safety and effectiveness of the RPS, and to make improvements necessary to improve rider safety, we examined a side load and a top load scenario. We used the Finite Element Analysis (FEA) simulation tool on SolidWorks to create a fine curvature-based mesh to test the max deformation of the RPS in these two scenarios.

2.1.2 Top Load Modeling: Methods and Assumptions

In accordance with the ASME rules, in the first scenario a top load of 2760 N (600 lbf) was applied at the top and center of the RPS, making a 12° angle with the vertical and pointing towards the back of the bike. This was done to simulate a rollover worst case scenario. The safety harness attachment points were assumed to be fixed in order to examine how the load affects the rider. The seat attachment and adjustment mechanism was assumed to be negligible and thus omitted, as it does not have any physical contact with the RPS. Despite the power of the SolidWorks FEA tool, the simulation is not perfect, and it does not account for imperfections due to welding, cutting, or other manufacturing processes, as well as the environmental and weather conditions during the competition. Thus, we were extremely conservative and aimed for a factor of safety (FOS) of no less than 5 to compensate for these imperfections.

2.1.3 Top Load Modeling: Results

After numerous trials testing different tube diameters and wall thicknesses for the RPS, it was found that using a 2" diameter tube with a 3/16" wall thickness resulted in a maximum deflection of 2.3 mm, which is well below 5.1 cm, as designated by ASME rules. This deflection also does not interfere with the rider's head or shoulders. This resulted in a FOS of 5.3, achieving our goal of at least 5. Refer to Appendix A for a comprehensive data table.

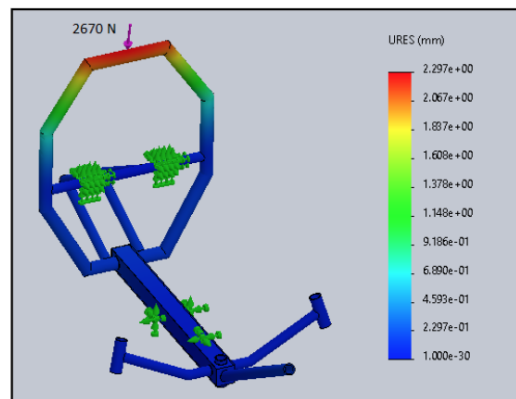


Fig. 11: Top load deflection using SolidWorks FEA analysis

2.1.4 Side Load Modeling: Methods and Assumptions

In accordance with the ASME rules, in the second scenario a side load of 1330 N (300 lbf) was applied to the side of the RPS at shoulder level. Again, this was done to simulate a rollover worst case scenario. The same assumptions were made as before about the safety harness attachment points being fixed, and the seat attachment/adjustment system not contacting the roll cage. We again aimed for a FOS no less than 5.

2.1.5 Side Load Modeling: Results

Using a 2" diameter tube with 3/16" wall thickness resulted in a maximum deflection of 0.55 mm, which is again well below the maximum deflection of 3.8 cm designated by ASME rules. This deflection will also not interfere with any part of the rider's body. Finally, the FOS in this case was 13, which is well above our goal of 5. The full results are in Appendix A.

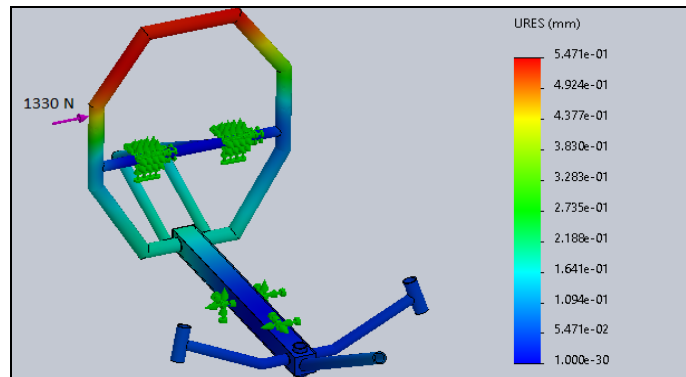


Fig. 12 Side load deflection using SolidWorks FEA analysis

2.1.6 Conclusions

The results show that by using aluminum tubing with a 2" diameter and 3/16" wall thickness, we can achieve a max deformation much less than the maximum allowable deformation per the ASME rules, as well as a high enough factor of safety to account for any errors during the manufacturing process or unpredictable environment conditions. This simulation also ignored any extra protection due to the fairing, which can be assumed to slightly absorb some of the impact. Thus, we claim that, despite the inability to do physical testing, our RPS is of the utmost safety for the competition and will provide sufficient protection for the rider.

2.2 Structural Analyses

We decided to do three structural analyses on the components of the bike which seemed most likely to fail; the results of these analyses allowed us to justify design choices. All structural analyses were done under the assumption that the rider weighs 180 lbs, the bike weighs 80 lbs, and the maximum speed of the bike is approximately 20 m/s (44.7 miles per hour). These specifications are our best approximations of the most failure-conductive reasonable scenario. The bike weight in particular is an upper bound since we cannot actually weigh the bike.

2.2.1 Main Horizontal Beam Stress Analysis

The first analysis we performed was a hand-calculation of the shear stress across the primary beam of the vehicle. Since the steering components are designed to go straight through this horizontal beam, we decided that it would be best to use a square-shaped beam instead of the typical circular beam, despite the significantly lower moment of inertia of the cross section. We decided to neglect the normal stress in the beam due to vehicle acceleration, because the shaft is much less likely to fail due to a reasonable quantity of tensile stress, and it would be negligible compared to the weight of the rider.

Table 11: Summary of Main Horizontal Beam Stress Analysis

Criteria	Description
Objective	Test safety of the main beam of the frame given forces acting on it during use
Method	Hand calculate the shear forces acting on the beam to determine if the beam will fail at any point
Final Result	Minimum factor of safety against yielding of 46

As seen in figure 13, we can simplify the system down to two reactions from the wheels and a loading consisting of four forces: the RPS and the three contact points between the main beam and the seat. We then assumed that the RPS weighed approximately 10 lbs, and the rider/seat weighed 200 lbs, half of which is on the front support and the other half of which is split evenly between the posterior supports. Summing the moments yields the respective reaction forces at the wheels (130 lbf on the rear wheel and 80 lbf on the front wheels).

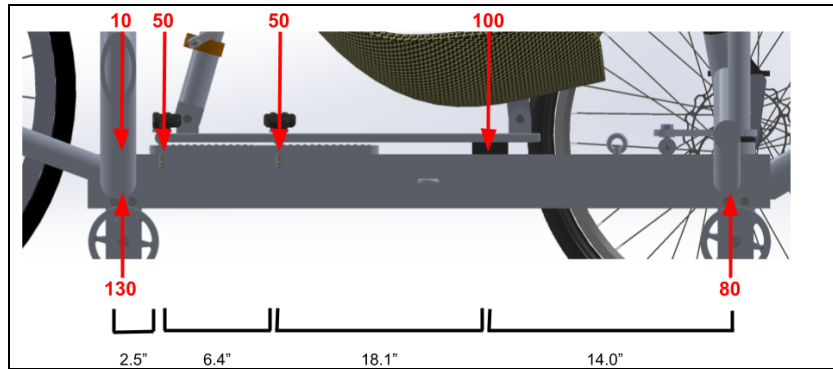


Fig 13: Shear Forces Acting on Main Beam

Thus, the maximum internal shear force that occurs in the beam is 120 lbf. Using our preferred cross section of a 3" x 3" square pipe with wall thickness $\frac{1}{8}$ ", we then calculated the maximum shear stress that the pipe would encounter. By the principles of solid mechanics, we know that

$$\tau = \frac{VQ}{It}$$

Plugging in the appropriate values yields a maximum internal shear stress of 375.2 psi, or 2.587 MPa. Since the material is 6061-T6 aluminum ($\delta_y = 240$ MPa), we can effectively apply the Tresca failure criterion for yielding, and our final factor of safety against yielding is approximately 46. Such a high factor of safety is more than enough to justify the decision to use a square cross section rather than the circular cross-section, even under the assumptions used in this analysis.

2.2.2 Back Seat Support Stress Analysis

Table 12: Summary of Back Seat Support Stress Analysis

Criteria	Description
Objective	Determine that the back seat support will not snap when the rider pedals to accelerate the bike.
Method	Stress analysis by hand
Final Result	Factor of safety against yielding of 52

Since the seat and rider are supported at just two points, a large amount of force must be transmitted through the back support while the rider is accelerating the bike to speed. Thus, we decided to do a stress analysis on the back beam just to make sure that it does not yield during use. For the sake of analysis, we decided to assume all of the weight of the rider and a 500 Newton (112 lbf) load due to pedalling were to be supported by the back support. Thus, the bar must be able to withstand 292 lbf. Since the support is pinned on both ends, it must be fully in compression under this load. If the beam fails, it will be at the thinner section of the beam with outer diameter 1.25" and inner diameter 1.00", yielding a cross-sectional area of .442 in². This means that the total normal stress endured by the support is 660.6 psi, or 4.555 MPa. Thus, we can conclude a factor of safety of 52 under monotonic loading conditions for 6061-T6 aluminum ($\delta_y = 240$ MPa), and the back support will not break while the rider accelerates the vehicle to speed.

2.2.3 Front Arms Finite Element Analysis

Table 13: Summary of Front Arms Stress Analysis

Criteria	Description
Objective	Test safety of the main beam of the front arms of the HPV given forces acting on it during use
Method	Solidworks FEA simulation
Final Result	Minimum factor against yielding of safety of 9

For this analysis of the main tube and the front arms we assumed an 80 lbf (355.8 N) applied to the main bar. After running a Solidworks FEA, shown in figure 14, we found that the factor of safety for the arm-main tube joint is 9. When treating the weld joint on the arm as one singular piece, we found the factor of safety to be considerably higher, approximately 60. Through this analysis, we are confident that a weld joint in the front arms is safe for the rider in operating the vehicle.

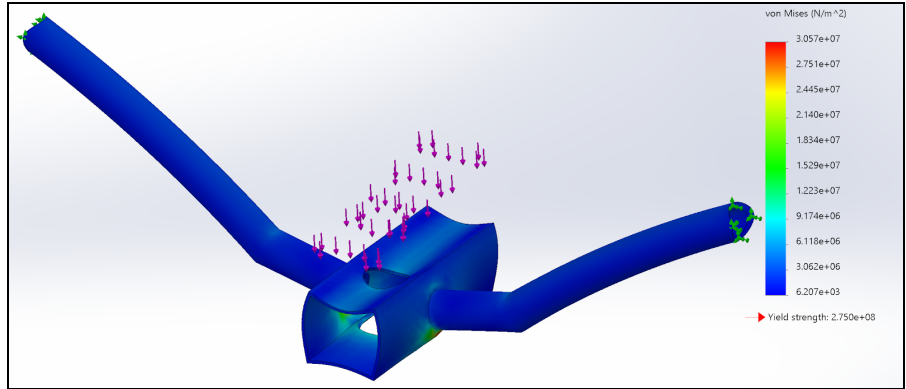


Fig 14: Front Arms FEA Results (exaggerated deflection)

2.3 Aerodynamic Analysis

Table 14: Summary of Aerodynamic Analysis

Criteria	Description
Objective	Verify that our design meets the previously determined design criteria ($C_d < 0.2$)
Method	Ansys Fluent CFD Simulation
Final Result	Estimated C_d of 0.1238

The goal of the aerodynamic analysis is to verify that our design meets the previously determined design criteria. One assumption taken in this analysis was that the simplified fairing is approximately representative of the drag coefficient of the entire vehicle. In reality, we understand that the other components likely contribute to increasing the drag coefficient. We also analyzed the bike at 30mph with no crosswinds and at STP. 30mph was selected as it is near the faster end of the spectrum in terms of speeds we reasonably expect to consistently reach. Using ANSYS Fluent simulations it was determined that the drag coefficient of the vehicle is expected to be 0.1238.

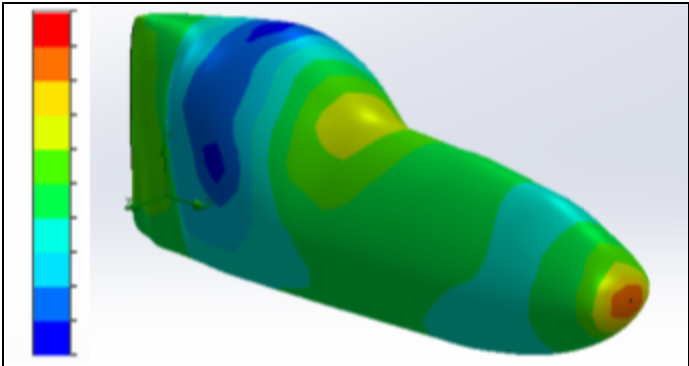


Fig 15: Graphical representation of the qualitative pressure distribution on the fairing

In evaluating other fairing styles (front or tail), we were unable to reduce the drag coefficient below or equal to that of our full fairing design. This makes sense as the full fairing design is

able to have greater freedom over the shape of the vehicle at the cost of a greater weight, so when properly designed it should almost always beat a front or tail fairing design when purely considering aerodynamic results.

2.4 Cost Analysis

This school year, 2020-2021, the school granted us a sum of \$11,493, \$8,000 of which we allocated for the theoretical production of HotDog.

Table 15: Categorical Costs of Production

Production Category	Cost
Capital Investments	\$135.76
Parts & Materials	\$7296.39
Tooling	\$0.00
Labor	\$110.00
Donated Parts, Material & Labor	\$0.00
Total	\$7542.15

To manufacture this bike our capital investments summed to \$135.76 which includes the costs of vacuum bagging materials as well as a cup gun machine. Both of these items will be used in creating the fairing. Our university supplies many of the tools and machines we would need in order to produce the bike free of charge, therefore expenses in capital investments and tooling is minimal. However, we do need to use a fraction of our budget for some labor costs which include heat treating the bike as well as transporting it via UHaul. The majority of our budget is allocated to buying parts for the bike which is broken down further in the next table and in Appendix E.

Table 16: Subteam Cost Breakdown

Category	Amount Spent	Percent of Parts Budget
Drivetrain	\$571.43	7.13%
Frame	\$1019.11	12.73%
Steering	\$820.17	10.25%
Fairing	\$4885.68	61.07%

This year our budget is approximately \$8000 to manufacture HotDog. As seen in the table above production of the fairing accounts for the majority of the budget, at 61.07%. A categorical breakdown of all of the sums by part cost and quantity from the table above can be found in Appendix E.

2.5 Other Analyses

2.5.1 Front Brake Mounts Finite Element Analysis

Table 17: Summary of Front Brake Mounts Stress Analysis

Criteria	Description
Objective	Test safety of the brake mounts during use
Method	SolidWorks FEA simulation (see below)
Final Result	Minimum factor of safety for yielding of 16 under idealized conditions

From the safety perspective, one of the most crucial parts of the vehicle is the brake mounts, pictured in figure 15. Since we designed this component to be machined ourselves, it is incredibly important that the brake mounts do not fail while at speed.

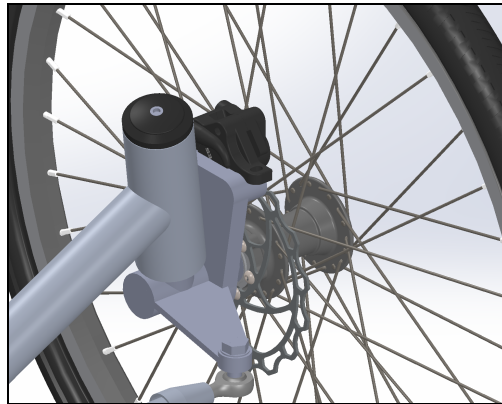


Fig 15: Brake Mount Flange

Using Newton's second law ($F = ma$) and a deceleration of 10 m/s^2 , a force of 590 Newtons must be applied to each of the two front wheels. This deceleration would be sufficient to bring the vehicle to a complete stop from the maximum speed of 20 m/s in 2 seconds. Since each flange has two pins, approximately 295 Newtons must be applied to each pin of the flange where the brake is mounted. Through Solidworks FEA, we found the factor of safety at the interface between the cylindrical shaft and the flange to be 16 under the assumption that they are one single combined piece. This factor of safety is high enough to be sure that the pieces will not split, even when the interface is replaced with the significantly weaker weld joint.

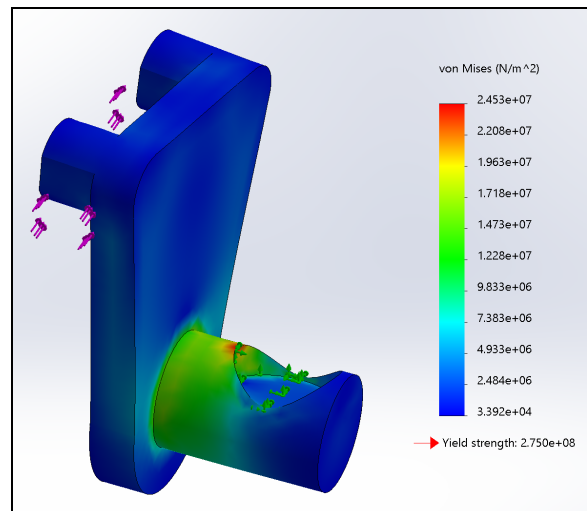


Fig 16: Brake Caliper Mount FEA Results

2.5.2 Steering Angles Analysis

Table 18: Summary of Steering Angle Analysis

Criteria	Description
Objective	Determine the steering geometry to make the steering system compatible with the fairing, while maintaining a 5 m minimum turn radius
Method	Hand calculations and SolidWorks working angle diagram
Final Result	Tie rod length reduced to 14" and handlebar width reduced to 9" to accommodate a 14° bell crank rotation

A key consideration when designing the steering mechanism for HotDog was to make sure that the steering system is fully compatible with the fairing and does not interfere with any other parts of the bike. Thus, a simple steering angle analysis was done to determine suitable steering geometry for a functional steering system. As given in Mark Archibald's textbook *Design of Human Powered Vehicles*, the theoretical turn angles for the inner and outer front wheel, using an Ackermann compensation, can be determined with the following equations:

$$\delta_i = \tan^{-1}\left(\frac{L}{R - \frac{T}{2}}\right) \quad \delta_o = \tan^{-1}\left(\frac{L}{R + \frac{T}{2}}\right)$$

Where L is the wheelbase, R is the minimum turn radius, and T is the kinematic track, or the distance between the base of the kingpins. The wheelbase was fixed at 51.3", and the turn radius was fixed at 196.9" (5 m). It is worth noting that as the turn angle of the wheels increases, the amount of error from the theoretical Ackermann angle will also increase (Archibald, 2016). However, due to the small size of these angles and lack of tight cornering required, we neglected the steering error, although it is something to examine in future testing.

The analysis was done in two parts. First, a kinematic track length was chosen and the turn angles were calculated using the above equations. Then we used a steering diagram on SolidWorks, which can be found in Appendix D, to determine the corresponding rotation of the bell crank. The angle that the bell crank rotates was assumed to be the angle that the handlebars must rotate to achieve the necessary turn angles.

In the end, the tie rod length was set at 14" (resulting in a 34" kinematic track), which is the minimum it could be without the kingpins running into the fairing. The corresponding steering angles are given in Table 19. Based on these angles, the handlebar length was shortened to 9 in. so as not to run into the fairing when turning.

Table 19: Calculated Steering Angles

Theoretical Inner Wheel Turn Angle	Theoretical Outer Wheel Turn Angle	Bell Crank and Handlebar Rotation
15.93°	13.50°	14.06°

3. CONCLUSION

3.1 Comparison-Design Goals and Analysis

Table 20: Design goals and results

Design Goals	Results
Stop from 25km/hr in 6 meters	Used disc brakes on all three wheels
Turn within an 8 m radius	Over seat dual drag linkage steering allows for 5 m turn radius
Stability at 5-8km/hr and start without assistance	Tadpole layout provides stationary stability and gearing is adequate to start from rest without assistance
Rollover protection system (RPS) can withstand 2760 N top force at a 12° angle from vertical with total deflection below 5.1 cm	Roll cage around shoulders able to withstand load with a factor of safety of 5.3 with a 2.3 mm deflection
RPS can withstand 1330 N side force with total deflection below 3.8 cm	Roll cage can withstand load with factor of safety of 15 with a 0.55 mm deflection
Vehicle must have a four or five point safety harness with minimum webbing width of 25 mm	Decided on a five point harness secured with an extra hole into the frame
Top speed 45 mph	Top speed of 50.47 mph achieved using the drivetrain system at 60 rpm cadence
Minimum factor of safety 5	Factors of safety for all loading analysis was above 5
Adjustable seat	Accomplished by designing a sliding and rotating adjustment mechanism
Lowest point of frame at least 7 in. above ground	Frame clearance is 7.9 in

3.2 Evaluation

The vehicle has met all of the analytical goals based on the design and the simulation tests that have been run. When compared to the competition objectives and design requirements of an effective vehicle, all the specified criteria have been met. Though the vehicle was unable to be built, the team feels confident about a manufactured vehicle based on the HotDog design succeeding in physical tests and competition events, while meeting all requirements.

3.3 Recommendations

More complex simulation tests involving the fairing and specified cases are recommended to allow for further confirmation of vehicle safety. In addition, being able to manufacture the vehicle in the future may be a great way to learn more lessons on improving the design for manufacturability. Harness attachment options will also be researched further to allow for effective safety systems while being integrated with structural frame parts. Finally, factors such as weight reduction, especially for the frame, may be further investigated in future iterations.

REFERENCES

Archibald, Mark. *Design of Human Powered Vehicles*. American Society of Mechanical Engineers

(ASME, 2016).

O'Brien, Mickey. "Types of Recumbent Trikes." *LaidBackCycles*.

<https://laidbackcycles.com/recumbent-types-tadpole-delta-trikes/#:~:text=Tadpole%20trikes%20tend%20to%20be,the%20short%20or%20distance%20riders.>

Horwitz, Rickey M. "The Recumbent Trike Design Primer." *Hell Bent Cycle Works*,

www.hellbentcycles.com/Trike%20Design%20101%20%20part-1.pdf.

Krider, Rob. "Installing A 5-Point Harness Properly." *TURNology*, 14 Mar. 2018,

www.turnology.com/tech-stories/chassis-safety/proper-5-point-harness-install/.

SDSU Human Powered Vehicle Team, "2019 ASME North HPVC Design Report." 5 Apr. 2019.

Too, Danny and Landwer, Gerald E., "The Biomechanics of Force and Power Production in Human Powered Vehicles" (2003). *Kinesiology, Sport Studies and Physical Education Faculty Publications*. 100. https://digitalcommons.brockport.edu/pes_facpub/100

UC Berkeley Human Powered Vehicle Team, "2018 ASME HPVC Design Report." 23 Mar. 2018.

Whitman, Alexander S. *A Systematic Approach to Human Powered Vehicle Design with an*

Emphasis on Providing Guidelines for Mentoring Students. 2016,

tigerprints.clemson.edu/cgi/viewcontent.cgi?article=3384&context=all_theses&httpsredir=1&referer=.

APPENDICES

Appendix A: Optimization of RPS Deflection and FOS

RPS Tube OD* (in.)	Wall Thickness (in.)	Total Weight of Frame (lbs)	Top Load Deflection (mm)	Top Load FOS	Side Load Deflection (mm)	Side Load min FOS
1.5	0.125 (1/8)	24.64	6.142	2.7	1.231	4.7
1.5	0.188 (3/16)	26.95	4.906	4	0.9949	6.8
1.5	0.25 (1/4)	29.01	4.284	4.8	0.8694	8.4
1.75	0.125 (1/8)	25.64	4.109	3.1	0.8712	7.7
1.75	0.188 (3/16)	28.43	3.247	4.9	0.7012	9.9
1.75	0.25 (1/4)	30.97	2.810	5.6	0.6097	13
1.75	0.313 (5/16)	33.27	2.535	6.4	0.5540	13
2.00	0.188 (3/16)	29.91	2.297	5.3	0.5471	13
2.00	0.25 (1/4)	32.95	2.069	6.5	0.4538	15

*Does not include RPS cross bar

Appendix B: Steering Geometry Table and Rationale

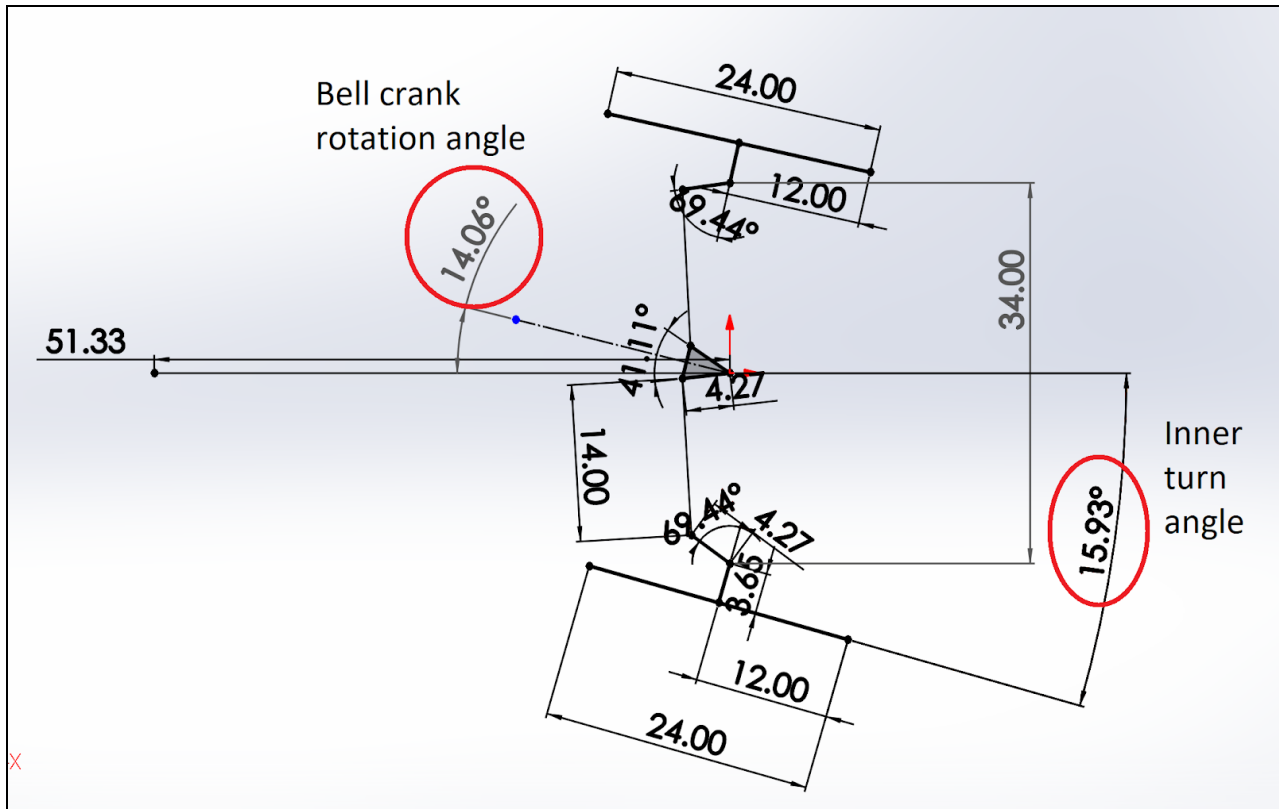
Steering Geometry Specification	Rationale
Kingpin angle 15°	Establish center point steering, allowing the tires to turn exactly on their contact point with the ground, reducing the amount of scrubbing and slippage.
Positive 10° caster angle*	Increase the force required to turn the front wheels, resulting in better control and handling.
Neutral camber*	Easier to manufacture given our steering knuckle and kingpin design, minimal tight cornering is required.

*Additional testing is needed to optimize this geometry. Further information can be found in Rickey Horwitz's *The Recumbent Trike Design Primer*

Appendix C: Measurements of Our Largest Driver

Measurement Definition	Dimension (Inches)
Top of head to base of neck	10
Shoulder to hip	21
Hip to knee	21
Knee to ankle	18
Shoulder to wrist	25
Width of shoulders	22
Width of hips	15
Overall Height	72

Appendix D: SolidWorks Steering Angle Diagram



Appendix E: Cost Analysis/ Part Breakdown

Category	Part Description	Price/ Unit	Quantity	Total
Drivetrain	Shimano 7/8 Speed Triple Crankset	\$74.72	1	\$74.72
	Shimano 7 Speed Internal Hub	\$179.57	1	\$179.57
	Shimano 16 Tooth Cog	\$9.48	1	\$9.48
	Front Derailleur	\$15.00	1	\$15.00
	Rear Tensioner	\$25.08	1	\$25.08
	8 Speed Chain	\$22.59	2	\$45.18
	Sport Idler Pulley	\$85	2	\$170
	Aluminum Sheet Metal (sq inches)	\$0.1	144	\$14.4
	Pack of 100 Washers	\$7.14	1	\$7.14
	Steel Setup Stud	\$1.31	2	\$2.62
	Black Oxide Alloy Steel Socket Head Screw	\$10.11	1	\$10.11
	M8 x 1.25mm Steel Hex Nut	\$5.09	1	\$5.09
	Pack of 100 ¼-20 Hex Nuts	\$4.88	1	\$4.88
	Pack of 100 ¼-20 ½ in Hex Screws	\$12.14	1	\$12.14
Frame	Fixtureworks Cam Lever	\$13.18	4	\$52.72
	Corki Quick Release Bicycle Seatpost Clamp	\$8.99	1	\$8.99
	2" OD 0.250" Wall Round Aluminum Tube (6' Length)	\$142.62	2	\$285.24
	1.5" OD .250" Wall Round Aluminum Tube (6' Length)	\$91.23	2	\$182.46
	.75" OD .5" ID Wall Round Aluminum Tube (10" long)	\$9.60	2	\$19.20
	14" x 2" x .5" Aluminum 6061 Block for long seat attachment pipe (Midwest Steel and Aluminum)	\$21.80	1	\$21.80
	5" x 3" x 5" Aluminum 6061 Block for brake caliper mount & miscellaneous machined parts (Midwest Steel and Aluminum)	\$33.55	1	\$33.55
	14" x 10" x .75" Aluminum 6061 Block for seat attachment plate (Midwest Steel and Aluminum)	\$64.24	1	\$64.24
	2" OD .375" Wall 6061-T6 Aluminum Tube (Length	\$53.06	1	\$53.06

	18")			
	BlueSunshine Aluminum Alloy Disc Brake + Calipers (set of 2)	\$24.99	1	\$24.99
	3" Sq .125" Wall 6063-T52 Aluminum Tube	\$126.49	1	\$126.49
Safety	Jegs High Performance Safety Harness	\$132.99	1	\$132.99
	Safety Harness Eye Bolts	\$4.49	3	\$13.47
Steering	Front Wheels (24")	\$37.99	2	\$75.98
	Back Wheel (29")	\$68.50	1	\$68.50
	Aluminum Stock (Bellcrank)	\$16.95	1	\$16.95
	Ball & Socket Joint	\$9.82	4	\$39.28
	Female Stud Tie Rod End	\$7.69	4	\$30.76
	.75" OD .125" Wall Aluminum Tube (Tie Rod)	\$14.17	1	\$14.17
	Handlebars Grips	\$4.99	1	\$4.99
	1 ¼ " OD 0.12" Wall 48" Inch Length (Steering Axle + Handlebars)	\$143.13	1	\$143.13
	3x7 Speed Brake/Shift Lever Set	\$31.99	1	\$31.99
	McMaster Steel Car U-Joint	\$328.05	1	\$325.05
	Headset	\$19.99	3	\$59.97
	Aluminum Tube Round 1 ¼ " OD .065" Wall 20" Length (Kingpin Spindles)	\$9.40	1	\$9.40
Fairing	Fairing Mold	\$4,000	1	~4,000
	Easy Sand	\$363.85	1	\$363.85
	FibreGlast (Epoxy)	\$521.83	1	\$521.83

Appendix F: Diagram of Body Joint Angles

